




Evaluation of Standardized MODIS-Terra Satellite-Derived Evapotranspiration Using Genetic Algorithm for Better Field Applicability in a Tropical River Basin

Utkarsh Kumar^{1,2}  · Rashmi³ · Ankur Srivastava⁴ · Nikul Kumari⁴ · Chandranath Chatterjee⁵ · Narendra Singh Raghuwanshi^{5,6}

Received: 26 July 2022 / Accepted: 7 February 2023 / Published online: 31 March 2023

© Indian Society of Remote Sensing 2023

Abstract

Evapotranspiration (ET) estimation at different spatial and temporal scales with a paucity of climatic parameters in a river basin is becoming a challenging task. Accurate estimation of ET is necessary for efficient water resource management and improving water efficiency at the field scale. Therefore, this study attempts to indirectly estimate actual ET from version 006 of MODIS-Terra product (MOD16A2.006), Sentinel-2A and Variable infiltration capacity (VIC-3L) model using survey information collected from a traditional paddy field in Kangsabati river basin. Further, this study is undertaken to standardize raw MODIS-Terra ET product (MOD16A2.06) using a genetic-based algorithm for better field applicability at local condition. The MODIS-standardized ET and ET estimated using different methods along with raw MODIS-Terra ET product were evaluated against observed ET estimated using globally recommended FAO-56 Penman–Monteith (PM) equation coupled with a crop coefficient. MODIS-Terra ET estimates were standardized using a genetic-based algorithm to enhance the efficacy of MODIS-Terra ET (MODIS-raw ET) for better field applicability. The result revealed that the genetic-based algorithm (MODIS-standardized ET) improved significantly with the NSE and RMSE from approximately -0.03 to 0.86 and 13.89 to 2.56 (mm/8 day). Of various ET models Sentinel-2A ET performed best followed by MODIS-standardized ET, VIC-3L ET and MODIS-raw ET with $R^2 = 0.92$, NSE = 0.89 , RMSE = 1.89 (mm/8 day), $R^2 = 0.88$, NSE = 0.86 , RMSE = 2.47 (mm/8 day), $R^2 = 0.77$, NSE = 0.76 , RMSE = 3.02 (mm/8 day) and $R^2 = 0.41$, NSE = -0.03 , RMSE = 7.31 (mm/8 day), respectively. The result showed that Sentinel 2A and MODIS-standardized-based ET can be used under data scarce conditions for better field applicability and water management practices.

Keywords Crop coefficient · Genetic algorithm · Penman-Monteith · Monteith · MODIS-Terra · Sentinel 2

✉ Utkarsh Kumar
utkarsh.kumar@icar.gov.in

¹ Crop Production Division, ICAR-Vivekananda Parvatiya Krishi Anusandhan Sansthan, Almora, Uttarakhand 263601, India

² Division of Agricultural Engineering, ICAR-Indian Agricultural Research Institute, New Delhi, Delhi 110012, India

³ Department of Agricultural Economics, Institute of Agricultural Sciences, Banaras Hindu University, Varanasi, Uttar Pradesh 221005, India

⁴ Faculty of Science, University of Technology Sydney, Sydney, NSW 2007, Australia

⁵ Agricultural and Food Engineering Department, Indian Institute of Technology Kharagpur, Kharagpur, West Bengal 721 302, India

⁶ Maulana Azad National Institute of Technology, Bhopal, 462 003, India

Introduction

About half of the precipitation received on the land surface is lost in the atmosphere as evapotranspiration, which makes it a vital hydrological component (Kumar et al., 2021a, 2021b, 2021c, 2021d, 2021e). Its accurate estimation is one of the biggest challenges in different regions of the globe due to various problems such as limited flux stations, expensive instruments and limited availability of open access data. Hence, it is very important to be precisely calculated under different available dataset conditions. In recent years, several satellite-based remote sensing (SBRS) models based on Landsat, Advanced Very High Resolution Radiometer (AVHRR), Moderate Resolution Imaging Spectroradiometer (MODIS), Sentinel, Himawari and (Syst&me Probatoire & Observation de la Terre) SPOT have

been evolved to estimate ET in different agro-climatic zones (Kumar et al., 2020; Kumari et al., 2021a, 2022). SBRS models furnish ET from the field, regional to basin scale with spatio-temporal variations, which has guided to a modern age in the estimation of irrigation water requirement (Tasumi et al., 2019). SBRS models are classified in three categories: vegetation indices-based, land surface-based and scatter plot/ triangle-based approaches (Biggs et al., 2016). Among different satellite-based ET estimation model Surface Energy Balance Algorithm for Land (SEBAL), Mapping Evapotranspiration at high Resolution with Internalized Calibration (METRIC), Surface Energy Balance System (SEBS) are the most popular methods (Allen 2007; Bastiaanssen et al., 1998; Su, 2002; Losgedaragh & Rahimzadegan, 2018; Kumar et al., 2022a, 2022b). All the above-mentioned methods are classified as land surface temperature-based models (Biggs et al., 2016). Several researchers across the globe have shown the capability for estimating ET using remote sensing at the farm to local scales (Allen, 2007; Bastiaanssen, 2000; Ray & Dadhwal, 2001). On the other hand catchment scale ET can be calculated by multiplying FAO-56-PM ET with normalized difference vegetation index (NDVI)-based crop coefficient. But such methodology is applicable for cloud-free days. Landsat or Advanced Spaceborne Thermal Emission and Reflection Radiometer (ASTER) produces ET estimate at a resolution of 30–100 m (Allen et al., 2011). The application of such satellite is not useful for agricultural purposes due to low temporal resolution. Therefore, there is a urgent need for a finer temporal resolution of 7–10 days for better management of irrigation requirements. The moderate resolution imaging spectroradiometer (MODIS) on board Terra and Aqua satellite produces fairly good ET estimates at different spatial and temporal resolutions (Anderson et al., 2011; Senay et al., 2013; Vinukolle et al., 2011).

Several authors have pointed out the efficacy of satellite-based ET estimation at different spatial and temporal scales with an ambiguity of 15–30% (Mu et al., 2007; Senay et al., 2008; Srivastava et al., 2021), which may increase up to 50% of the total average annual ET values for coarse-resolution scale (Glenn et al., 2011). Therefore the assessment of coarse-resolution data has been a prime topic. There are limited studies regarding the evaluation of ET calculated from MODIS-Terra ET product (MOD16A2.06), MODIS-enhanced vegetation index (EVI) and MODIS land surface temperature (LST) with reference to benchmark FAO-56-PM ET estimation model. The current approach applied for estimating ET at the catchment scale is either based on the use of the land surface model forced with weather data or the surface energy balance model. The soil and water assessment tool (SWAT) estimates ET based on the hydrological response unit (HRU) without sub-grid scale variability of soil

moisture and land use land cover (LULC), which may result in a discrepancy in estimating ET. Several other hydrological models such as variable infiltration capacity (VIC) have been applied to test the applicability of the MODIS products, however, limited to its validation with fine-resolution satellites (Srivastava et al., 2021; Kumar et al., 2021c; Kumar et al., 2021e). The aforesaid review reveals that standardized MODIS-ET product is not evaluated against FAO-56-PM-based ET in a tropical river basin. Ruhoof et al. (2013) reported that MODIS-ET product does not perform well in wet climate.

To address the above research gaps, the aim of the present research is 1) to estimate ET using different algorithms (Sentinel-2A based ET, MODIS-Terra ET product and VIC-3L), 2) to standardize MODIS-Terra satellite derived ET using a genetic-based algorithm, 3) to evaluate the performance of ET estimated using four models against the standard FAO-56-PM-based method.

Project Site Description and Data Used

The project site selected for evaluation of standardized MODIS-ET is Kangsabati River Basin (KRB) (Fig. 1). The geographic extent of KRB with longitude (86°E–87°30'E) and latitude (22°20'N–23°30'N) has a total area of 5796 km². The terrain of study area varies from 11 to 656 m above mean sea level. Rice is the dominant crop grown in the command area throughout the year (Kharif, Rabi and summer) and works as local agent for ET loss (Fig. 2). The climate of KRB is tropical–monsoon type. The basin receives average annual rainfall of about 1400 mm, while approximately 80% of normal rainfall is

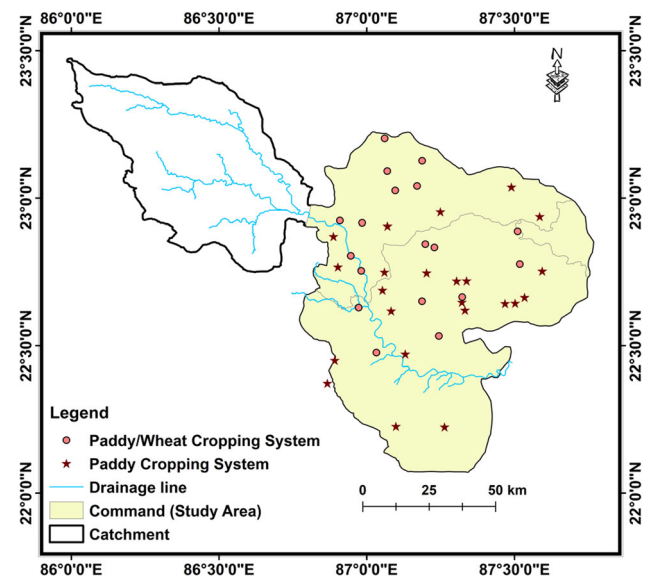
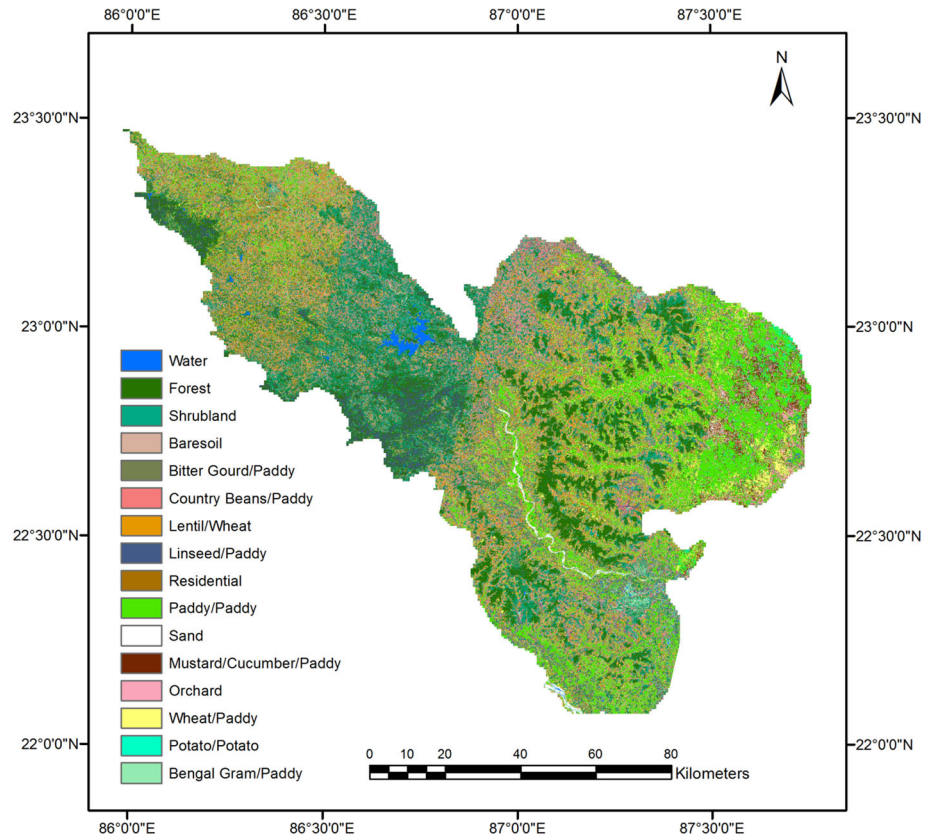


Fig. 1 Location of the study area showing survey location recorded during field campaign

Fig. 2 Land use/land cover map of the Kangsabati command area which shows 16 different landuse/landcover classes. Adapted from Maza et al. (2020)



in monsoon season (June to September). The Kangsabati reservoir irrigation project is located at the confluence of the Kangsabati and Kumari Rivers (Kumar et al., 2021c, 2021e). Two dams were established in 1965 and 1974, respectively, to mitigate the flooding situations in the command area. The KRB has been conventionally considered as drought prone.

Remotely Sensed Data

The MOD16A2.06 Terra ET product having spatial resolution of 500 m and temporal resolution of 8 days was utilized (http://files.ntsg.umd.edu/data/NTSG_Products/MOD16/). The algorithm for computing ET_o is based on the PM equation. In addition to this, Sentinel-2A imagery was acquired from the Copernicus Sentinel-2 satellite. Two similar satellites those were launched on June 23, 2015 (Sentinel-2A), and on March 7th, 2017 (Sentinel-2B), constitute a constellation. For optimal coverage and data distribution, both satellites were orbiting apart at 180° at an altitude of 786 km. Sentinel-2 provides better data, especially in temporal and spatial resolution compared to other moderate spatial resolution satellite (e.g., Landsat). It has 13 bands having spatial resolution ranging from 10 to 60 m. The spectral and spatial characteristics of the MSI (Multispectral Instrument) sensor of the Sentinel-2A and 2B satellites used in the study are given in Table 1. The

10-m spatial resolution in visible and near-infrared (NIR) bands makes Sentinel imagery to have potential use for study of agriculture-related activities. These bands represent minimum and maximum values of reflection and absorption of chlorophyll in vegetation therefore NDVI selected. The other most important useful characteristic of Sentinel-2 imagery is its 5-day temporal resolution. Sentinel-2 data are freely available, making it simple for resource-constrained researchers to use it and supplement it with other freely available data such as Landsat.

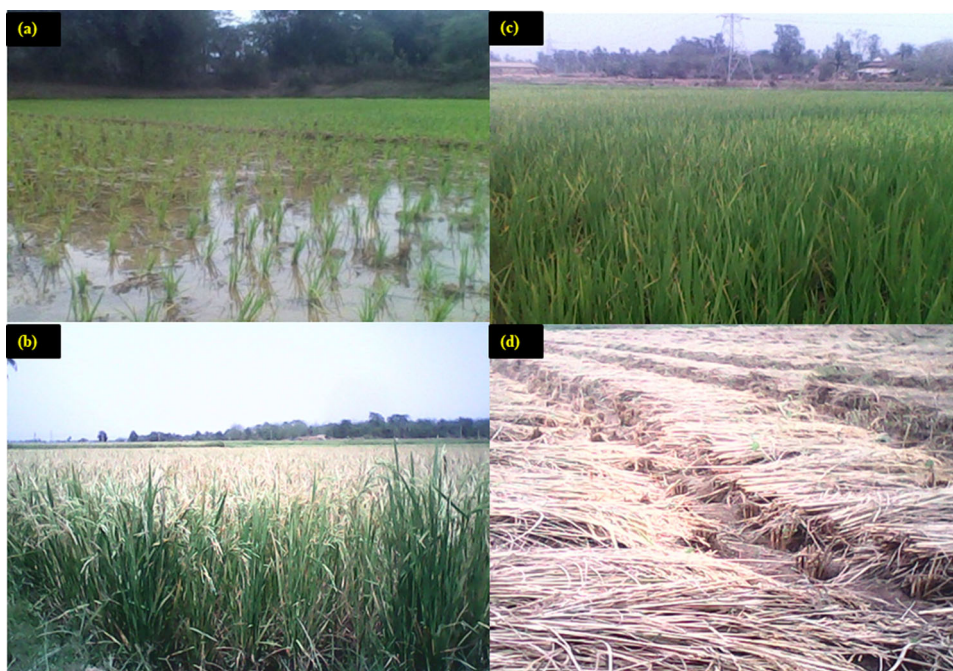
Survey Data for Crop Coefficient Vegetation Modeling

For calculating crop coefficient (K_c) a survey was conducted to know the crop characteristics parameter such as sowing date, latitude, longitude, crop type, crop height. Survey data for crop coefficient vegetation modeling were collected from 100 survey points for Rabi season during (January–April) covering the KRB. Due to variations in the crop characteristics throughout its growing season, K_c for a given crop changes from sowing till harvest. The typical information for a survey location during different growth stage is given in Fig. 3 along with corresponding detailed description given in Table 2. Survey data points were collected from a traditional paddy field having large field of homogeneous land use/land cover (LULC). Survey data

Table 1 Spectral and spatial characteristics of the MSI (Multispectral Instrument) sensor of the Sentinel-2A and 2B satellites

Spectral band		Wavelength (μm)	Spatial resolution (m)
B2	Blue (B)	0.459–0.525	10
B3	Green (G)	0.542–0.578	
B4	Red (R)	0.650–0.680	
B8	Near-infrared (NIR)	0.781–0.887	
B5	Red edge 1 (Re1)	0.697–0.712	20
B6	Red edge 2 (Re2)	0.733–0.748	
B7	Red edge 3 (Re3)	0.773–0.793	
B8A	Near-infrared narrow (NIRn)	0.856–0.876	
B11	Shortwave infrared 1 (SWIR1)	1.569–1.660	
B12	Shortwave infrared 2 (SWIR2)	2.115–2.290	
B1	Coastal aerosol	0.433–0.453	60
B9	Water vapor	0.935–0.955	
B10	Cirrus	1.359–1.390	

Fig. 3 Variation of crop characteristics during **a** initial stage, **b** crop development stage, **c** mid-season stage, **d** maturity stage



included facts such as land use categories, crop type, sowing date, crop height, irrigation source and latitude and longitude of the field using a global positioning system (GPS). Attempts were made to select the survey date coinciding with the satellite visit period.

Meteorological Data

For determining the crop coefficient, an experiment was carried out in the experimental field of Indian Institute of Technology (IIT), Kharagpur, Agricultural and Food Engineering department (AgFE), having geographic location ($23^{\circ} 32' \text{ N}$; $87^{\circ} 31' \text{ E}$) during the rabi season. Six non-

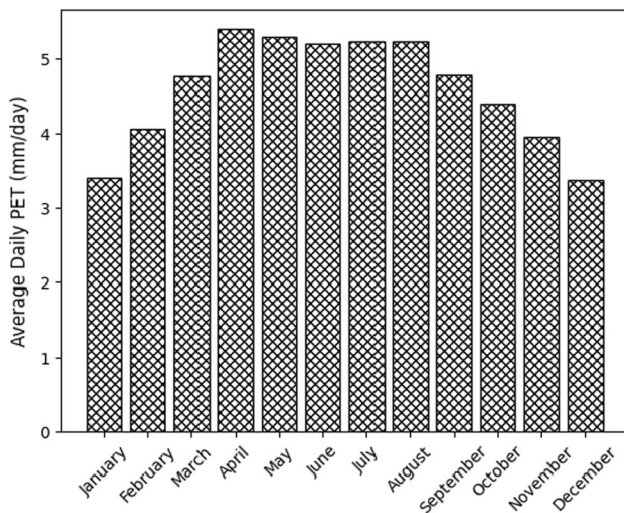
weighing lysimeter out of which (4 open bottom and 2 closed bottom) were installed with/without paddy having dimension of $1.25 \text{ m} \times 1.25 \text{ m} \times 6 \text{ m}$. Water balances approaches based on volumetric basis in the open bottom and closed bottom were used to calculate crop evapotranspiration (ET) on daily basis. Consequently daily crop coefficients were by taking the ratio of ET_c to FAO-56 PM-derived ET_o of rabi season and aggregated to mean for different crop growth stage. The crop coefficient value of rice rabi, rice kharif, rice summer and wheat for study area from various literature is given in Table 3. Average daily ET_o variations in different month are shown in Fig. 4.

Table 2 Detailed description of crop information and geolocation of Fig. 2

Description	Fig. (a)	Fig. (b)	Fig. (c)	Fig. (d)
Sub-division	Jhargram	Jhargram	Jhargram	Jhargram
Village	Chunapra	Chunapra	Chunapra	Chunapra
Area	1 Bigha	1 Bigha	1 Bigha	1 Bigha
Plot latitude	22° 13' 35.8" N	22° 13' 35.8" N	22° 13' 35.8" N	22° 13' 35.8" N
Plot longitude	87° 05' 56.4" E	87° 05' 56.4" E	87° 05' 56.4" E	87° 05' 56.4" E
Crop	Paddy	Paddy	Paddy	Paddy
Date of sown	Mid-Jan	Mid-Jan	Mid-Jan	Mid-Jan
Date of harvest	Mid-April	Mid-April	Mid-April	Mid-April
Primary water source	Shallow tube well	Shallow tube well	Shallow tube well	Shallow tube well
Secondary water source	Rainfed	Rainfed	Rainfed	Rainfed
Growth description	3	15	25	Harvested

Table 3 Crop coefficient value for paddy and wheat at different growth stage in the study area

Crop	Initial	Crop development	Mid-season	Maturity	Reference
Paddy kharif	1.05	1.25	1.01	0.89	Srivastava et al. (2017)
Paddy rabi	0.92	1.02	1.08	0.88	Srivastava et al. (2017)
Paddy summer	1.05	1.2	1.15	0.8	Srivastava et al. (2017)
Wheat	0.33	0.82	1.08	0.64	Bandyopadhyay and Mallick (2003)

**Fig. 4** Monthly mean daily PET variation during (2016–2020) in the study area

Methodology

Calculation of Crop ET

The methodological flowchart of the entire analysis and processing of the datasets used in this study is shown in

Fig. 5. Reference ET is calculated using Penman–Monteith model from climate data available from weather station located in IIT Kharagpur, which is located in the command area. The meteorological site receives an average annual rainfall of 156.4 cm, annual minimum and maximum temperatures of 12 °C and 40 °C, respectively, and humidity of 46–98%. The average annual solar radiation and wind speed are 197.7 W/m² and 2.78 km/h, respectively. Crop evapotranspiration is calculated as:

$$ET_c = K_c \times ET_o. \quad (1)$$

There are different equations developed to estimate ET_o across the globe in different agro-climatic zone and extensively evaluated using lysimeter data. However, the standard and reliable method for computing ET_o is FAO Penman–Monteith (Allen et al., 1998; Kumar et al., 2022a). In the present study we have used to FAO Penman–Monteith method to calculate ET_o . The reference ET is computed using climate parameter and represents the response of climate parameter on environmental condition. K_c is different for different crops and represents the crop canopy development and crop management practices through the growing season. The FAO-56-PM method was employed as a reference method in the present investigation.

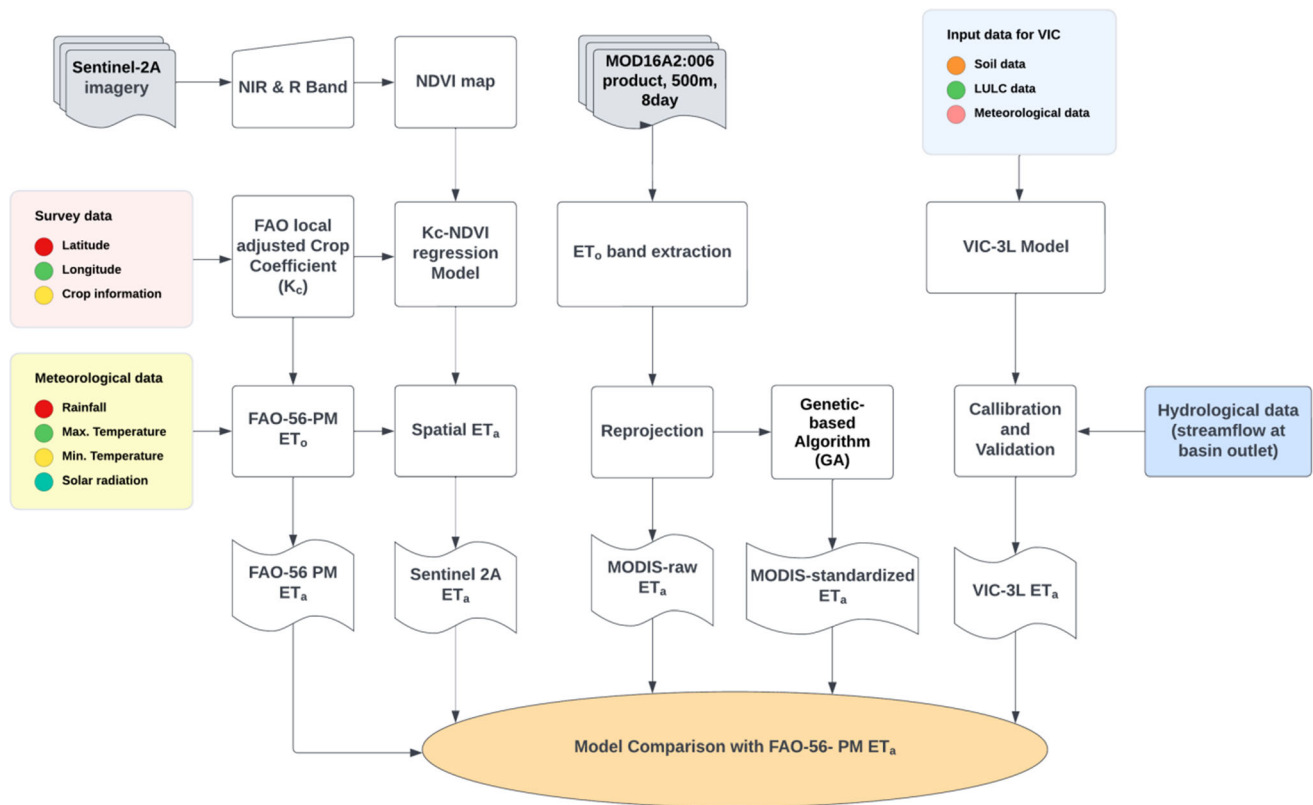


Fig. 5 Applied methodology flowchart for evaluation of ET_a using different models

$$ET_o = \frac{0.408(R_n - G) + \frac{900}{T_a + 273} u(e_s - e_a)}{\Delta + \gamma(1 + 0.34u)} \quad (2)$$

where ET_o is the potential reference crop evapotranspiration (mm day^{-1}); R_n is the total incoming solar radiation ($\text{MJ m}^{-2} \text{day}^{-1}$); G is the ground heat flux ($\text{MJ m}^{-2} \text{day}^{-1}$), which is taken as nil on a daily basis; T_a is the mean daily temperature ($^{\circ}\text{C}$); u is the wind speed at a height of 2 m (m s^{-1}); e_s is the vapor pressure deficit at saturation (kPa); e_a is the vapor pressure deficit of actual air (kPa); $e_s - e_a$ is the difference in vapor pressure deficit (kPa); Δ is the tangent of the saturation vapor pressure–temperature curve ($\text{kPa } ^{\circ}\text{C}^{-1}$); and γ is constant of psychometric ($\text{kPa } ^{\circ}\text{C}^{-1}$).

Computation of FAO Adjusted Crop Coefficient

At different phases of crop growth, several crop characteristics parameters were employed to compute the K_c (Doorenbos and Pruitt 1977). Crop type, sowing and harvesting dates, and growth stage were measured using a field survey conducted at 100 locations during the Rabi season of 2014–2015 (November 2014 to March 2015). This comprehensive verification of agricultural land use crops is supported by previous research and produced good ET estimation results (Kumari & Srivastava, 2020; Srivastava

et al., 2017; Zhang et al., 2001). The tabulated crop-specific K_c values were directly taken from FAO-56 manual (Allen et al., 1998) and were adjusted for local crop condition as

$$K_{c(\text{modified})} = K_{c(\text{table})} + [0.04(u_2 - 2) - 0.004(\text{RH}_{\min} - 45)] \left(\frac{h}{3}\right)^{0.3} \quad (3)$$

where $K_{c(\text{table})}$ is the value of crop coefficient given in Table 12 of FAO-56 manual (Allen et al., 1998), RH_{\min} is the mean minimum relative humidity value for a particular stage (%) for $20\% \leq \text{RH}_{\min} \leq 80\%$, h is crop height from survey information for particular stage (m) for $0.1 \text{ m} < h < 10 \text{ m}$, and u_2 is the value of wind at the height of 2 m.

Crop Coefficient Model Development Using Vegetation Index Approach

Sentinel-2A-based ET (Sentinel-ET) was calculated using FAO Penman–Monteith method (FAO-56 PM) cum crop coefficient vegetation regression model by processing Sentinel-2 data in conjunction with field survey data and meteorological data in the study area. Crop coefficient (K_c) is an important parameter, which is defined as the ratio of

ET_c/ET_o used for calculation of ET crop-related information along with their latitude and longitude collected using survey data to calculate K_c value and for developing VI- K_c model. The K_c value for different survey locations (Fig. 1) was calculated during distinct crop growth phase of the Rabi season (2014–2015). Attention were given while selecting the survey location to prevent mixing of pixels; the plot size having greater than 30 m × 30 m was taken under consideration. NDVI maps were created for each pass of the study area during the study period. For each survey location NDVI values were extracted for calculation of K_c value from crop information and adjusted to local condition using Eq. (3). The idea behind developing the VI- K_c model is to express the crop coefficient as a function of NDVI. The general form of the VI- K_c model to be applied to satellite imagery can be expressed as (Kamble et al., 2013)

$$K_c(\text{VI}) = C_1 \times \text{NDVI} + C_2 \quad (4)$$

where C_2 and C_1 are the intercept and slope, respectively; its value was estimated through least square regression. The value of C_1 and C_2 coefficients is unique for each crop; therefore, a regression model for different crop should be developed separately using their corresponding NDVI and K_c value. The above developed regression model showed that NDVI (vegetation cover) is directly proportional to the crop coefficient. K_c map was generated for each satellite imagery, and corresponding ET_o was multiplied to get the actual evapotranspiration of the given date. The potential ET was determined using the global recommended method. The value of the coefficient of determination fluctuates from 0 to 1, and it is used to determine the degree of fit between the dependent and independent variables. The lowest and highest value represents no fit and perfect fit, respectively, for the VI- K_c model shown in Eq. (5).

$$R^2 = \left[\frac{\sum_{i=1}^n (K_c - \bar{K}_c)(\text{NDVI} - \overline{\text{NDVI}})}{\sum_{i=1}^n \sqrt{(K_c - \bar{K}_c)^2 (\text{NDVI} - \overline{\text{NDVI}})^2}} \right]^2 \quad (5)$$

It is used to represent the proportion of variability in K_c that may be associated with the linear combination of independent variables. Crop characteristics information was an essential parameter used for developing VI- K_c regression model.

MODIS-Derived ET Estimation

In this section, a methodology for the estimation of terrestrial ET from the MODIS-Terra satellite product was utilized which is applied globally (Mu et al., 2007, 2011; Srivastava et al., 2017; Kumari and Srivastava 2020). ET is calculated in three partitions, where it includes evaporation

from the canopy, transpiration from vegetation and evaporation from the soil moisture. The basic algorithm of the MODIS-ET estimation is based on the Penman–Monteith equation which is given as follows

$$ET = \frac{LH}{\lambda} = \frac{E(de_{\text{sat}}/dT) + \rho C_p (e_{\text{sat}} - e)r_a}{\lambda \left[(de_{\text{sat}}/dT) + \gamma \left(1 + \frac{r_s}{r_a} \right) \right]} \times \text{PET} \quad (6)$$

where LH is latent heat flux; λ is $(2.501 - 0.002361Ta_n) \times 10^6$; Ta_n is the air temperature at every half hourly; PET is potential evapotranspiration, E is the amount of energy which is divided among the latent heat, soil heat and sensible heat fluxes, r_a and ρ are aerodynamic resistance and density of air, respectively, C_p and p are specific heat capacity of air and psychrometric constant as shown in Eq. 8 (Maidment, 1993). Further, de_{sat}/dT is the gradient which relates between saturated water vapor pressure (e_{sat}) and temperature (T); e is the vapor pressure which varies at a different rate per unit time and r_s is the surface resistance

$$p = \frac{C_p P_a M_d}{\lambda M_w} \quad (7)$$

where M_w and M_d are wet and dry molecular masses of air, respectively, and P_a is atmospheric pressure. Surface resistance is explained as the actual resistance from the surface of the land and the actual transpiration from canopy layer. This algorithm is modified and is the unique state-of-the-art method to estimate the actual ET from different vegetation and biomes at various timescales such as 8 days, monthly and annual scales. At all the scales this product has been verified from different biomes as well as for different climatic regions yielding high accuracy of ET estimates (Srivastava et al., 2017).

The MODIS-ET used in this study is MOD16A2.006 which computes ET as a summation of evaporation from the wet soil, intercepted canopy precipitation and ET in night-time using vegetation cover fraction, stomatal and aerodynamic conductance, etc., which is given as (Mu et al., 2011)

$$ET = E_c + T_d + E_b \quad (8)$$

$$\text{PET} = E_{\text{wc}} + T_p + E_w + E_p \quad (9)$$

where ET is daily ET, E_c is the evaporation from the moist the canopy surface; T_d is transpiration from canopy surface which is dry, E_b is bare soil evaporation, T_{pdc} is potential transpiration from the dry canopy surface, E_w is wet soil evaporation, and E_p is potential soil evaporation. The soil heat flux (G) is used for calculation of soil evapotranspiration during day and night. A detailed explanation of the entire MOD16A2 algorithm and its pre-processing is described in Mu et al. (2011); readers are encouraged for further reading. For using the MOD16A2 the projection of

the projection was converted into the Universal Transverse Mercator for further pre-processing of the datasets as in the raw format it is in sinusoidal and type of file is hierarchal data format (.hdf). A detailed description of the processing can be found in Degano et al. (2021).

Standardization of MODIS-ET Using Genetic Algorithm

The MODIS-Terra ET (MODIS-raw) product is not free from bias. Hence before using this product it has to be standardized using PM-based ET estimates as Eq. (11)

$$\hat{ET}_{M,j\Delta t} = ET_{M,j\Delta t} + \hat{\varepsilon}_{j\Delta t} \quad (10)$$

$$\hat{\varepsilon}_{j\Delta t} = a \left(ET_{M,j\Delta t} - \hat{ET}_{PM,j\Delta t} \right)^c + b \cos(\beta \cdot j\Delta t + \varphi) + \delta \quad (11)$$

where $\hat{ET}_{M,j\Delta t}$ = standardized MODIS-derived ET at ($j\Delta t$) time step (mm = day); $ET_{M,j\Delta t}$ = MODIS-raw derived ET at ($j\Delta t$) time step (mm = day); $\hat{\varepsilon}_{j\Delta t}$ = predicted bias at ($j\Delta t$) time step (mm = day); $\hat{ET}_{PM,j\Delta t}$ = FAO-56 PM-derived ET estimates at ($j\Delta t$) time step (mm = day); Δt = revisit period of MODIS-Terra satellite (= 8 days); ϕ = phase difference (day); and a , b , c , β and δ are the fitting constants. The six parameters a , b , c , β , ϕ and δ are evaluated by using the GA by minimizing the mean-square error between $\hat{ET}_{M,j\Delta t}$ and $ET_{M,j\Delta t}$.

Genetic algorithm (GA) is a stochastic optimization technique in evolutionary research. It is represented by a fixed-length bit string. The position of every individual element in the string represents its feature, and the value associated with a particular element represents how that feature is exhibited in the solution. The analogy of GA is inspired from the natural selection. It utilizes a variety of operator during the search operation. Selection is one of the most important processes in GA that tells whether a particular string will participate in the reproduction process or not. Evaluation process comprises different generation; string selection; string crossover; and random mutation. The GA is having a length of 16-bit chromosome-specific elitist evolution algorithm.

Performance Indicator

To compare the accuracy level of ET_c calculated by different models (MODIS-raw, MODIS-standardized, Sentinel-2A and VIC-3L) with the standard FAO-56-PM-based ET statistical analysis was performed. Statistical analyses for the evaluation were: the coefficient of determination

(R^2), Eq. (12); root-mean-squared error (RMSE), Eq. (13); and Nash–Sutcliffe efficiency (NSE), Eq. (14):

$$R^2 = \frac{[(\sum_{i=1}^n (P_i - \bar{P})(O_i - \bar{O}))]^2}{[\sum_{i=1}^n (P_i - \bar{P})^2][\sum_{i=1}^n (O_i - \bar{O})^2]} \quad (12)$$

$$RMSE = \sqrt{\frac{\sum_{i=1}^n (P_i - O_i)^2}{n}} \quad (13)$$

$$NSE = 1 - \frac{\sum_{i=1}^n (O_i - P_i)^2}{\sum_{i=1}^n (O_i - \bar{O})^2} \quad (14)$$

where O_i is the observed ET_c (mm/day) values calculated from FAO-56 PM equation; P_i is the estimated ET_c (mm/day) by the model; \bar{O} is the average observed ET_c value; n is the number of observations.

Results and Discussion

Standardization of MODIS-ET Product

MOD16A2.006 product provides data with a spatial resolution of 500 m and corresponding to 8-day accumulated values. To process this product, first, we downloaded the product (http://files.ntsng.umd.edu/data/NTSG_Products/MOD16/); then, we extracted ET_o band; after that, we re-projected the product with “MODIS conversion toolkit” in geographic information system (GIS) environment for visualizing imagery (ArcGIS). Genetic-based algorithm is applied for bias correction of MOD16A2.006 product. The fitting parameters of optimization function Eq. (11) for 8-day ET standardization are $a = 1.526$, $b = 0.8935$, $c = 0.3638$, $\beta = 30.31$, $\varphi = -65.68$ and $\delta = 1.8583$ mm/day. As depicted from Figs. 6 and 7 standardized MODIS-ET performed well on 8 days and monthly scale for the study area during 2016–2020.

Temporal Variation of ET Using Different Algorithms

The temporal variation of ET for the study period using different ET algorithms over KRB is represented in Fig. 6. The typical spectrum for monthly ET profile during a year is represented in Fig. 7. The results revealed that the MODIS-raw ET values are highly underestimated during the study period with some phase differences. After standardization of these ET estimates by the genetic-based algorithm, the performance of the MODIS-standardized ET improved significantly with the NSE and RMSE (mm/8 day) from approximately – 3% to 86% and 7.31 to 2.47. The rising part of ET profile curve marks the initial stage of crop growth. From the temporal ET profile it is clear that

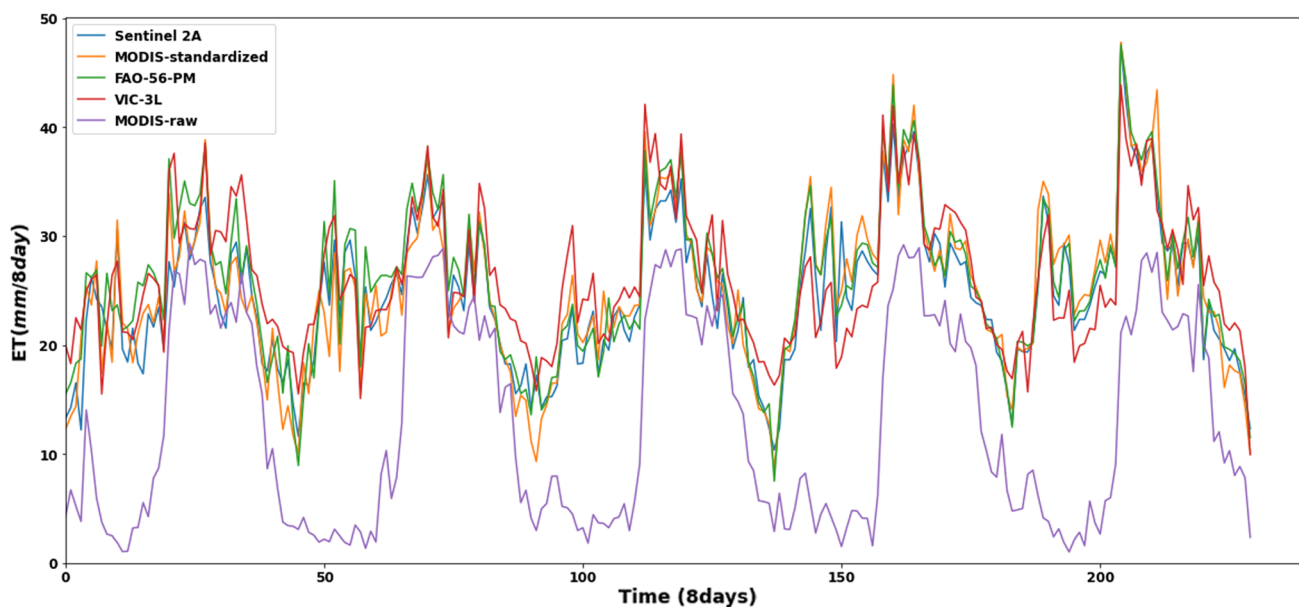
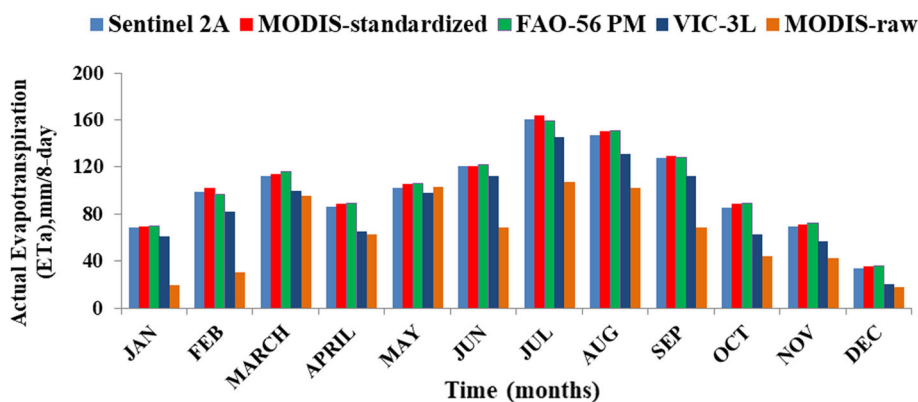


Fig. 6 Average temporal profiles of ET (mm/8 days) for study area using different algorithms during (2016–2020)

Fig. 7 Average monthly daily reference evapotranspiration (ET_o) at study area for the study period



ET is maximum in July and August and minimum in winter. The forest land cover has a large amount of ET in comparison with crop land.

Comparison of ET Algorithm with FAO-56-PM Model

ET estimated from different methods (VIC-3L, MODIS-raw, MODIS-standardized and Sentinel 2A-based ET) was compared by benchmark FAO-56-PM-based ET by taking 8 daily scale (Fig. 8). When comparing MODIS-raw ET data with FAO-56-PM data, the results show an overestimation, as shown in Fig. 8a, with a NSE value around -3%. The results found in this study are comparable to those obtained by several authors in different regions for MOD16A2.006 product (Autovino et al., 2016; Chang et al. 2018; Hu et al., 2015; Ruhoff et al., 2013). The

statistical error suggests that MOD16A2.006 product is not suitable for estimating ET_o directly; hence, it is imperative to correct the raw MOD16A2.006 product using a genetic-based algorithm. After correction, the errors decrease significantly (Table 4), and product results improve considerably (Fig. 8c). The result showing improvement in ET estimation after applying correction is corroborated by the findings of Degano et al. (2021). The Sentinel-2A ET performed well with observed PM-based estimates with $R^2 = 0.92$, NSE = 0.89 and RMSE = 1.89 (mm/8 day) as shown in Fig. 7b, while MODIS-raw-based ET performed worst with $R^2 = 0.41$, NSE = -0.03 and RMSE = 7.31 (mm/8 day) (Fig. 8a). The comparison result reveals that the ET values estimated after applying correction, i.e., MODIS-standardized, could be satisfactorily used for regional and grid scale variability of evapotranspiration

Fig. 8 Scatter plot **a** MODIS-raw, **b** Sentinel-2A, **c** MODIS-standardized, **d** VIC-3L versus FAO-56-PM ET

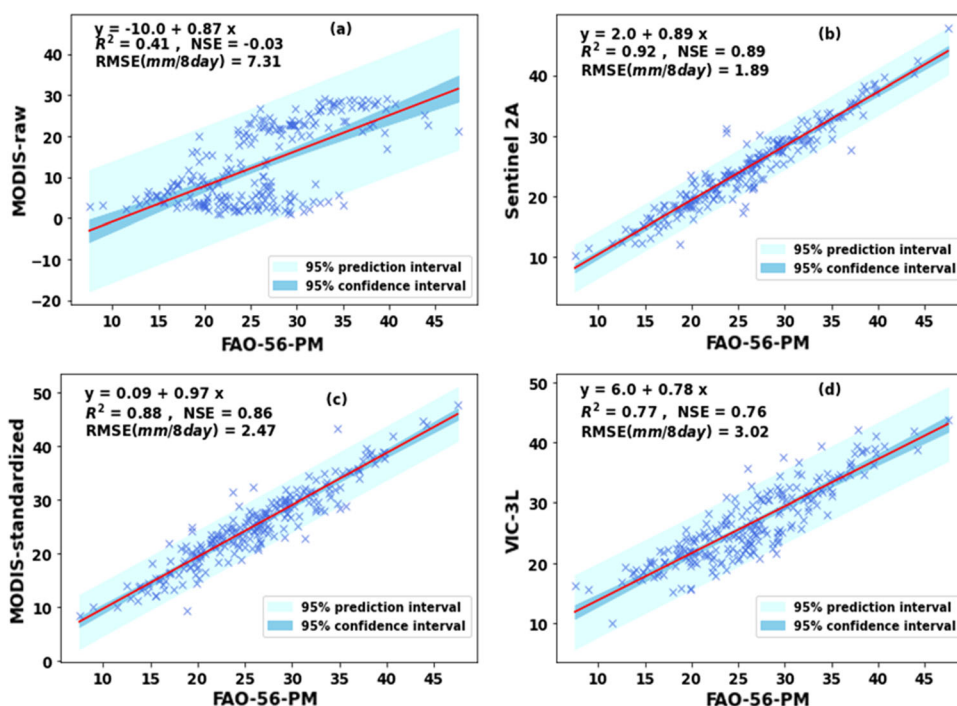


Table 4 Statistical metrics for MOD16A2.006 (MODIS-raw ET) and corrected MOD16A2.006 (MODIS-standardized ET) against benchmark FAO-56-PM-based ET

Statistics (mm/8 day)	MODIS-raw ET	MODIS-standardized ET
RMSE	7.31	2.47
NSE	-0.03	0.86
R^2	0.41	0.88

estimation when the field scale measured data are not available.

Conclusions

The present manuscript standardized the MOD16A2.006 product using a genetic-based algorithm and its evaluation against recommended FAO-56-PM-based actual ET for enhancing the field applicability. After applying this correction, we obtain appropriate potential evapotranspiration values for its application and use in different field of studies (hydrology, agricultural, meteorology). It is concluded that, given the existence of systematic error, it is required a correction to the MOD16A2.006 product in the KRB region before using data directly. Taken together, our collective analysis and evaluation of four evapotranspiration models, i.e., (Sentinel-2A-based ET, MODIS-raw, MODIS-standardized and VIC-3L) Sentinel-2A-based ET provides more accurate estimation than standardized

MODIS-Terra ET and VIC-3L estimates. The findings of this study are encouraging for the execution of calculation of crop water requirement in the command area. It can be used as a monitoring tool for near-real-time application in irrigation water management. Using the results, it is feasible to promote efficient water management practices that can reduce the risk of water stress during the critical growth period and recurrent heat spells during summer. This can effectively reduce the wastage of irrigation water by avoiding extra irrigation of grasslands and facilitate better methodology to reduce energy and water consumption. The study can be applied to rice-growing agricultural-dominated countries such as parts of the world such as China, Bangladesh, Indonesia, Thailand, USA and many more. The limitation of the investigation is that it holds good suitability in energy limited ecosystems; however, for other ecosystems further investigation is required.

Acknowledgements This work is carried at IIT Kharagpur at Geographic Information System (GIS) laboratory group under Professional Attachment Training (PAT). We acknowledge the Ministry of Human Resources Development, IIT Kharagpur as well as Indian Council of Agricultural Research (ICAR), New Delhi, and ICAR-Vivekananda Parvatiya Krishi Anusandhan Sansthan, Almora 263601 for providing financial support during PAT. We also acknowledge the Agricultural and Food Engineering Department, IIT Kharagpur, for providing necessary technical facilities during the course of investigation.

Funding Not applicable.

Data Availability The authors confirm that the data supporting the findings of this study are available within the article.

Declarations

Conflict of interest No potential competing interest was reported by the authors.

Ethics Approval and Consent to Participate Not applicable.

Consent for Publication Not applicable.

References

- Allen, R. G. (2007). Satellite-based energy balance for mapping evapotranspiration with internalized calibration (METRIC)—Application. *Journal of Irrigation and Drainage Engineering*. [https://doi.org/10.1061/\(ASCE\)0733-9437\(2007\)133:4\(380\), 380-394](https://doi.org/10.1061/(ASCE)0733-9437(2007)133:4(380), 380-394).
- Allen, R. G., Pereira, L. S., Howell, T. A., & Jensen, M. E. (2011). Evapotranspiration information reporting. I: Factors governing measurement accuracy. *Agricultural Water Management*, 98(6), 899–920. <https://doi.org/10.1016/j.agwat.2010.12.015>.
- Allen, R. G., Pereira, L. S., Raes, D., & Smith, M. (1998). Crop evapotranspiration: Guidelines for computing crop water requirements. FAO Irrigation and Drainage Paper No. 56, Food and Agriculture Organization of the United Nations.
- Anderson, M. C., Kustas, W. P., Norman, J. M., Hain, C. R., Mecikalski, J. R., Schultz, L., González-Dugo, M. P., Cammalleri, C., d'Urso, G., Pimstein, A., & Gao, F. (2011). Mapping daily evapotranspiration at field to continental scales using geostationary and polar orbiting satellite imagery. *Hydrology Earth System Sciences*, 15, 223–239. <https://doi.org/10.5194/hess-15-223-2011>.
- Autovino, D., Minacapilli, M., & Provenzano, G. (2016). Modelling bulk surface resistance by MODIS data and assessment of MOD16A2 evapotranspiration product in an irrigation district of Southern Italy. *Elv. Agricultural Water Management*, 167, 86–94. <https://doi.org/10.1016/j.agwat.2016.01.006>.
- Bandyopadhyay, P. K., & Mallick, S. (2003). Actual evapotranspiration and crop coefficients of wheat (*Triticum aestivum*) under varying moisture levels of humid tropical canal command area. *Agricultural Water Management*, 59, 33–47. [https://doi.org/10.1016/S0378-3774\(02\)00112-9](https://doi.org/10.1016/S0378-3774(02)00112-9).
- Bastiaanssen, W. G. M. (2000). SEBAL-based sensible and latent heat fluxes in the irrigated Gediz Basin, Turkey. *Journal of Hydrology*, 229, 87–100. [https://doi.org/10.1016/S0022-1694\(99\)00202-4](https://doi.org/10.1016/S0022-1694(99)00202-4).
- Bastiaanssen, W. G. M., Menenti, M., Feddes, R. A., & Holtslag, A. A. M. (1998). A remote sensing surface energy balance algorithm for land (SEBAL): 1. Formulation. *Journal of Hydrology*, 212–213, 198–212. [https://doi.org/10.1016/S0022-1694\(98\)00253-4](https://doi.org/10.1016/S0022-1694(98)00253-4).
- Biggs, T. W., Petropoulos, G. P., Velpuri, M. N., Marshall, M., Glenn, E. P., Nagler, P., & Messina, A. (2016). Remote sensing of actual evapotranspiration from croplands. Remote Sensing Handbook In P. S. Thenkabail (Ed.), *Remote sensing of water resources, disasters, and urban studies* (Vol. III, pp. 59–100). CRC Press.
- Chang, Y., Qin, D., Ding, Y., Zhao, Q., & Zhang, S. (2018). A modified MOD16 algorithm to estimate evapotranspiration over alpine meadow on the Tibetan Plateau, China. *Journal of Hydrology*, 561, 16–30. <https://doi.org/10.1016/j.jhydrol.2018.03.054>.
- Degano, M. F., Rivas, R. E., Carmona, F., Niclos, R., & Sanchez, J. M. (2021). Evaluation of the MOD16A2 evapotranspiration product in an agricultural area of Argentina, the Pampas region. *Egyptian Journal of Remote Sensing and Space Sciences*, 24(2), 319–328. <https://doi.org/10.1016/j.ejrs.2020.08.004>.
- Doorenbos, J., & Pruitt, W. O. (1977). Guidelines for prediction of crop water requirements. FAO Irrigation and Drainage Paper No. 24 (revised), Food and Agricultural Organization of the United Nations.
- Glenn, E. P., Neale, C. M. U., Hunsaker, D. J., & Nagler, P. L. (2011). Vegetation index-based crop coefficients to estimate evapotranspiration by remote sensing in agricultural and natural ecosystems. *Hydrological Processes*, 25, 4050–4062. <https://doi.org/10.1002/hyp.8392>.
- Hu, G., Jia, L., & Menenti, M. (2015). Comparison of MOD16 and LSA-SAF MSG evapotranspiration products over Europe for 2011. *Remote Sensing Environment*, 156, 510–526. <https://doi.org/10.1016/j.rse.2014.10.017>.
- Kamble, B., Kilic, A., & Hubbard, K. (2013). Estimating crop coefficients using remote sensing-based vegetation index. *Remote Sensing*, 5(4), 1588–1602. <https://doi.org/10.3390/rs5041588>.
- Kumar, U., Meena, V. S., Singh, S., Bisht, J. K., & Pattanayak, A. (2021a). Evaluation of digital elevation model in hilly region of Uttarakhand: A case study of experimental farm Hawalbagh. *Indian Journal of Soil Conservation*, 49, 77–81. <https://doi.org/10.54302/mausam.v72i2.622>.
- Kumar, U., Panday, S. C., Kumar, J., Meena, V. S., Parihar, M., Singh, S., Bisht, J. K., & Kant, L. (2021b). Comparison of recent rainfall trend in complex hilly terrain of sub-temperate region of Uttarakhand. *Mausam*, 72(2), 349–358. <https://doi.org/10.3390/su132413786>.
- Kumar, U., Panday, S. C., Kumar, J., Parihar, M., Meena, V. S., Bisht, J. K., & Kant, L. (2022a). Use of a decision support system to establish the best model for estimating reference evapotranspiration in sub-temperate climate: Almora, Uttarakhand. *Agricultural Engineering International: CIGR Journal*, 24(1), 41–50. <https://doi.org/10.5772/intechopen.107920>.
- Kumar, U., Rashmi, R., Chatterjee, C., & Raghuwanshi, N. S. (2021c). Comparative evaluation of simplified surface energy balance index-based actual ET against lysimeter data in a tropical river basin. *Sustainability*, 13, 13786. <https://doi.org/10.1007/s12040-021-01622-1>.
- Kumar, U., Rashmi, R., Singh, D. K., Panday, S. C., Parihar, M., Bisht, J. K., & Kant, L. (2022b). Trend analysis of streamflow and rainfall in the Kosi River Basin of Mid-Himalaya of Kumaon Region, Uttarakhand. In R. Ray, A. P. D. G. Panagoulia, & N. Abeyingha (Eds.), *River basin management—Under a changing climate*. InTech Open: London. <https://doi.org/10.5772/intechopen.107920>.
- Kumar, U., Sahoo, B., Chatterjee, C., & Raghuwanshi, N. (2020). Evaluation of simplified surface energy balance index (S-SEBI) method for estimating actual evapotranspiration in Kongsabati reservoir command using Landsat 8 imagery. *Journal of Indian Society of Remote Sensing*, 48, 1421–1432. <https://doi.org/10.1007/s12524-020-01166-9>.
- Kumar, U., Singh, S., Bisht, J. K., & Kant, L. (2021d). Use of meteorological data for identification of agricultural drought in Kumaon region of Uttarakhand. *Journal of Earth System Sciences*, 130, 121. <https://doi.org/10.1007/s12524-021-01367-w>.
- Kumar, U., Srivastava, A., Kumari, N., Rashmi, R., Sahoo, B., Chatterjee, C., & Raghuwanshi, N. S. (2021e). Evaluation of spatio-temporal evapotranspiration using satellite-based approach and lysimeter in the agriculture dominated catchment. *Journal of Indian Society of Remote Sensing*, 49, 1939–1950.
- Kumari, N., & Srivastava, A. (2020). An Approach for estimation of evapotranspiration by standardizing parsimonious method.

- Agricultural Research*, 9, 301–309. <https://doi.org/10.1007/s40003-019-00441-7>.
- Kumari, N., Srivastava, A., & Dumka, U. C. (2021a). A long-term spatiotemporal analysis of vegetation greenness over the Himalayan Region using Google Earth Engine. *Climate*, 9(7), 109. <https://doi.org/10.3390/cli9070109>.
- Kumari, N., Srivastava, A., & Kumar, S. (2022). Hydrological analysis using observed and satellite-based estimates: Case study of a lake catchment in Raipur, India. *Journal of the Indian Society of Remote Sensing*, 50(1), 115–128. <https://doi.org/10.1007/s12524-021-01463-x>
- Kumari, N., Srivastava, A., Sahoo, B., Raghuvanshi, N. S., & Bretreger, D. (2021b). Identification of suitable hydrological models for streamflow assessment in the Kangsabati River Basin, India, by using different model selection scores. *Natural Resources Research*, 30(6), 4187–4205. <https://doi.org/10.1007/s11053-021-09919-0>.
- Losgedaragh, S. Z., & Rahimzadegan, M. (2018). Evaluation of SEBS, SEBAL, and METRIC models in estimation of the evaporation from the freshwater lakes (Case study: amirkabir dam, Iran). *Journal of Hydrology*, 561, 523–531. <https://doi.org/10.1016/j.jhydrol.2018.04.025>.
- Maidment, D. R. (1993). *Handbook of hydrology*. McGraw-Hill.
- Maza, M., Srivastava, A., Bisht, D. S., Raghuvanshi, N. S., Bandyopadhyay, A., Chatterjee, C., & Bhadra, A. (2020). Simulating hydrological response of a monsoon dominated reservoir catchment and command with heterogeneous cropping pattern using VIC model. *Journal of Earth System Science*, 129(1), 1–16. <https://doi.org/10.1007/s12040-020-01468-z>.
- Mu, Q., Heinsch, F. A., Zhao, M., & Running, S. (2007). Development of a global evapotranspiration algorithm based on MODIS and global meteorology data. *Remote Sensing Environment*, 111(4), 519–536. <https://doi.org/10.1016/j.rse.2007.04.015>.
- Mu, Q., Zhao, M., & Running, S. W. (2011). Improvements to a MODIS global terrestrial evapotranspiration algorithm. *Remote Sensing Environment*, 115(8), 1781–1800. <https://doi.org/10.1016/j.rse.2011.02.019>
- Ray, S., & Dadhwal, V. (2001). Estimation of crop evapotranspiration of irrigation command area using remote sensing and GIS. *Agricultural Water Management*, 49(3), 239–249. [https://doi.org/10.1016/S0378-3774\(00\)00147-5](https://doi.org/10.1016/S0378-3774(00)00147-5).
- Ruhoff, A. L., Paz, A. R., Aragao, L. E. O. C., Mu, Q., Malhi, Y., Collischonn, W., Rocha, H. R., & Running, S. W. (2013). Assessment of the MODIS global evapotranspiration algorithm using eddy covariance measurements and hydrological modelling in the Rio Grande basin. *Hydrological Sciences Journal*, 58(8), 1658–1676. <https://doi.org/10.1080/02626667.2013.837578>.
- Senay, G. B., Bohms, S., Singh, R. K., Gowda, P. H., Velpuri, N. M., Alemu, H., & Verdin, J. P. (2013). Operational evapotranspiration mapping using remote sensing and weather datasets?: A new parameterization for the SSEB approach. *Journal of the American Water Resources Association*, 49(3), 577–591. <https://doi.org/10.1111/jawr.12057>.
- Senay, G. B., Verdin, J. P., Lietzow, R., & Melesse, A. M. (2008). Global daily reference evapotranspiration modeling and evaluation. *Journal of American Water Resource Association*, 44(4), 969–979. <https://doi.org/10.1111/j.1752-1688.2008.00195.x>.
- Srivastava, A., Deb, P., & Kumari, N. (2020a). Multi-model approach to assess the dynamics of hydrologic components in a tropical ecosystem. *Water Resource Management*, 34, 327–341. <https://doi.org/10.1007/s11269-019-02452-z>.
- Srivastava, A., Kumari, N., & Maza, M. (2020b). Hydrological response to agricultural land use heterogeneity using variable infiltration capacity model. *Water Resource Management*, 34, 3779–3794. <https://doi.org/10.1007/s11269-020-02630-4>.
- Srivastava, A., Rodriguez, J. F., Saco, P. M., Kumari, N., & Yetemen, O. (2021). Global analysis of atmospheric transmissivity using cloud cover, aridity and flux network datasets. *Remote Sensing*, 13(9), 1716. <https://doi.org/10.3390/rs13091716>.
- Srivastava, A., Sahoo, B., Raghuvanshi, N. S., & Chatterjee, C. (2018). Modelling the dynamics of evapotranspiration using Variable Infiltration Capacity model and regionally calibrated Hargreaves approach. *Irrigation Sciences*, 36, 289–300. <https://doi.org/10.1007/s00271-018-0583-y>.
- Srivastava, A., Sahoo, B., Raghuvanshi, N. S., & Singh, R. (2017). Evaluation of variable-infiltration capacity model and MODIS-terra satellite-derived grid-scale evapotranspiration estimates in a River Basin with Tropical Monsoon-Type climatology. *Journal of Irrigation and Drainage Engineering*, 143(8), 04017028. [https://doi.org/10.1061/\(ASCE\)IR.1943-4774.0001199](https://doi.org/10.1061/(ASCE)IR.1943-4774.0001199).
- Su, Z. (2002). The Surface Energy Balance System (SEBS) for estimation of turbulent heat fluxes. *Hydrology Earth System Sciences*, 6, 85–100. <https://doi.org/10.5194/hess-6-85-2002>.
- Tasumi, M., Moriyama, M., & Shinohara, Y. (2019). Application of GCOM-C SGLI for agricultural water management via field evapotranspiration. *Paddy Water Environment*, 17, 75–82. <https://doi.org/10.1007/s10333-019-00699-1>.
- Vinukollu, R. K., Meynadier, R., Sheffield, J., & Wood, E. F. (2011). Multi-model, multi-sensor estimates of global evapotranspiration: Climatology, uncertainties and trends. *Hydrological Processes*, 25(26), 3993–4010. <https://doi.org/10.1002/hyp.8393>.
- Zhang, L., Dawes, W. R., & Walker, G. R. (2001). Response of mean annual evapotranspiration to vegetation changes at catchment scale. *Water Resource Research*, 37(3), 701–708. <https://doi.org/10.1029/2000WR900325>.

Publisher's Note Springer Nature remains neutral with regard to jurisdictional claims in published maps and institutional affiliations.

Springer Nature or its licensor (e.g. a society or other partner) holds exclusive rights to this article under a publishing agreement with the author(s) or other rightsholder(s); author self-archiving of the accepted manuscript version of this article is solely governed by the terms of such publishing agreement and applicable law.